Residual stress measurement of fiber texture materials near single crystal

Proceedings of the Seventeenth (2007) International Offshore and Polar Engineering Conference
Lisbon, Portugal, July 1-6, 2007

ISBN 978-1-880653-68-5; ISBN 1-880653-68-0(Set); ISSN 1098-6189 (Set)

Residual Stress Measurement of Fiber Texture Materials Near Single Crystal

Toshiya MORI, Masahide GOTOH**, Toshihiko SASAKI*** and Yukio HIROSE*****

*Graduate school of Natural Science and Technology, Kanazawa University
**Venture Business Laboratory, Kanazawa University
***Department of Materials Scinece and Enginering, Kanazawa University
****Department of Risk Base System Enginerring, Kanazawa University
Kanazawa, Ishikawa, Japan

ABSTRACT

In this paper, a sample having <111> fiber texture near single crystal structure made by PVD was evaluated about texture states by the pole figure and about residual stress states by the new expression for X-ray stress analysis. As a result, about 6GPa compressive residual stress existed in the film. However, measurement planes of X-ray line were influence on each stress value.

KEY WORDS: Residual stress; single crystal; texture; X-ray.

INTRODUCTION

X-ray stress measurement methods can measure surface stresses in polycrystalline ceramics and metals without destruction. However this method cannot be applied to anisotropy materials, because it is on the assumption of heterogeneous material in theoretical expression (Noyan and Cohen, 1987). Some researchers have proceeded to develop new procedures applied to fiber texture materials. Zaouali et al. (1991) discussed a measurement technique by using the procedure defined as the ideal orientation. Some groups also discussed the influences on stress determination of the elastic constant (Miki et al., 2000; Ejiri et al., 2000; Tanaka et al., 2000; Scardi and Dong, 2001). In addition, naturally, the new experimental techniques of stress measurement of textured materials were discussed also by some groups (Ma et al., 2001). On the other hand some researchers have studied about X-ray stress measurement of single crystals (Suzuki et al., 2000; 2003; Brückner et al., 2005). About these theories for stress measurements, they assume that materials have ideal orientation. However all materials are not always such extremity condition naturally. Some of the authors studied on the stress measurement of fiber-textured materials (Murotani et al., 2000; Ejiri et al., 2000). The specimens had very strong fiber texture in that study. On the other hand, it is known that the thin films that consisted of the single crystal structure can produce by PVD. The specimen having the intermediate structure between the single crystal and the fiber-textured crystal were obtained in this study. In this case, the X-ray stress-strain relation that related to the stress constant should be different between the single crystal and the fiber texture. Therefore, final objective of this research aims at development of stress measurement method for non-ideal orientation system near single crystal.

In this study, the residual stresses of a specimen having fiber texture near single crystal are investigated by procedures for ideal orientation. A sample having <111> fiber texture near single crystal structure was evaluated from the pole figure. Then, the residual stresses were measured by using several stress determinant procedures. One of the procedures is for the single crystal model, and others are for the ideal fiber texture model. At first, in this paper, authors introduce the principal expression of X-ray stress analysis and modify those equations to the procedures. The procedures were applied in the experiments using a strong textured sample. Experimental results obtained by these procedures were compared and discussed.

DETERMINATION OF X-RAY STRESS ANALYSIS

X-ray stress-strain relation of single cubic crystal and iso-biaxial stress state

The orthogonal coordinate systems used in the following determination are shown in Figure 1. The axes of the specimen coordinate system P define the surface of the specimen, and P_3 axis decides normal direction of specimen surface. The axes of the laboratory coordinate system L are defined as a coordinate system after it is converted by angle ϕ and ψ from P system. Then L_3 is in the direction normal to the family of planes (*hkl*) whose spacing is measured by X-ray. The axes of the crystal coordinate system C defined along their primitive axes. Figure 2 shows the relation between three coordinate systems. The laboratory coordinate system L can be transformed from the specimen coordinate system P. The transformation matrix ω_{ij} is given with rotation angle ϕ and ψ.

$$\omega_{ij} = \begin{pmatrix} \cos\psi\cos\phi & \cos\psi\sin\phi & -\sin\psi \\ -\sin\phi & \cos\phi & 0 \\ \sin\psi\cos\phi & \sin\psi\cos\phi & \cos\psi \end{pmatrix}. \quad (1)$$

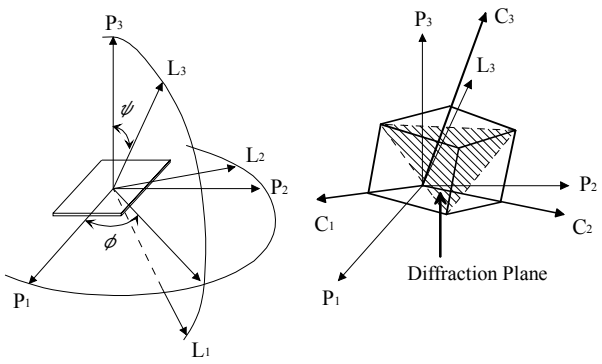

Fig.1 Orthogonal coordinate system.

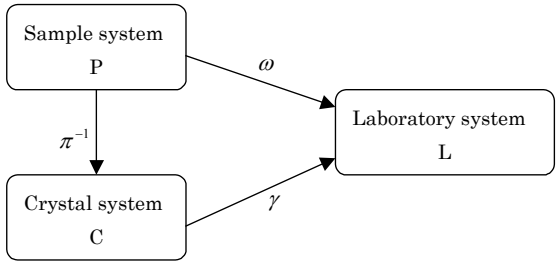

Fig.2 Relation between three coordinate system.

In the crystal coordinate system, the relation between the strain $\varepsilon_{ij}^{\mathrm{C}}$ and the stress σ_{ij}^{C} is expressed by

$$\varepsilon_{ij}^{\mathrm{C}} = S_{ijkl}^{\mathrm{C}} \sigma_{kl}^{\mathrm{C}} . \tag{2}$$

The strain measured by X-ray diffraction $\varepsilon_{33}^{\mathrm{L}}$ is the normal strain in the L_3 direction. Here, the relation between the strain $\varepsilon_{33}^{\mathrm{L}}$ and the strain $\varepsilon_{ij}^{\mathrm{C}}$, and the relation between the stress σ_{kl}^{C} and the stress σ_{ij}^{P} are given respectively by transformation of coordinate as follows:

$$\varepsilon_{33}^{\mathrm{L}} = \gamma_{3i}\gamma_{3j}\varepsilon_{ij}^{\mathrm{C}} , \tag{3}$$

$$\sigma_{ij}^{\mathrm{C}} = \pi_{ki}\pi_{lj}\sigma_{kl}^{\mathrm{P}} . \tag{4}$$

By the equation 2, 3 and 4, the relation between the strain and the stress is expressed by

$$\varepsilon_{33}^{\mathrm{L}} = \gamma_{3i}\gamma_{3j} S_{ijkl}^{\mathrm{C}} \pi_{mk}\pi_{nl}\sigma_{mn}^{\mathrm{P}} , \tag{5}$$

where the indexes are applied the Einstein suffix. γ_{ij} is the transformation matrix from C system to L system, and π_{ij} is from C to P, respectively. S_{ijkl}^{C} is the compliance moduli of the crystal (Kittel, 1996). In the case of the cubic crystal, it can be expressed by using only three components, S_{11}^{C}, S_{12}^{C} and S_{44}^{C}. Here, S_{ab}^{C} is indicated using Voigt notation. Finally, the relation between the X-ray strain $\varepsilon_{33}^{\mathrm{L}}$ and the stress σ_{ij}^{P} has following form:

$$\varepsilon_{33}^{\mathrm{L}} = (S_0^{\mathrm{C}} M_{ij} + S_{12}^{\mathrm{C}}\delta_{ij} + \frac{1}{2} S_{44}^{\mathrm{C}} \omega_{3i}\omega_{3j})\sigma_{ij}^{\mathrm{P}} , \tag{6}$$

$$S_0^{\mathrm{C}} = S_{11}^{\mathrm{C}} - S_{12}^{\mathrm{C}} - \frac{1}{2} S_{44}^{\mathrm{C}} , \tag{7}$$

$$M_{ij} = \sum_{t=1}^{3} \gamma_{3t}\gamma_{3t}\pi_{it}\pi_{jt} , \tag{8}$$

where δ_{ij} is Kronecker's symbol. Here, ω_{3i} is expressed by the equation of coordinate system transformation as

$$\omega_{3i} = \gamma_{3t}\pi_{it} . \tag{9}$$

Assuming that iso-biaxial stress state is applied in equations 6, 7 and 8, the equation of X-ray stress-strain relation of single cubic crystal is given by

$$\frac{\varepsilon_{33}^{\mathrm{L}}}{\sigma^{\mathrm{P}}} = S_{11}^{\mathrm{C}} + S_{12}^{\mathrm{C}} - \left[S_0^{\mathrm{C}} \sum_{t=1}^{3} (\gamma_{3t}\pi_{3t})^2 + \frac{1}{2} S_{44}^{\mathrm{C}} (\sum_{t=1}^{3} \gamma_{3t}\pi_{3t})^2 \right] , \tag{10}$$

where γ_{3t} and π_{3t} can be calculated by the direction cosine.

$$(\gamma_{31}, \gamma_{32}, \gamma_{33}) = \frac{1}{\sqrt{h^2 + k^2 + l^2}} (h, k, l) . \tag{11}$$

$$(\pi_{31}, \pi_{32}, \pi_{33}) = \frac{1}{\sqrt{H^2 + K^2 + L^2}} (H, K, L) , \tag{12}$$

where, H, K, L is the axis of fiber texture respectively. In the case of <111> fiber textured material, equation 10 is described using equation 12 as

$$\frac{\varepsilon_{33}^{\mathrm{L}}}{\sigma^{\mathrm{P}}} = S_{11}^{\mathrm{C}} + S_{12}^{\mathrm{C}} - \frac{1}{3} S_0^{\mathrm{C}} - \frac{1}{6} S_{44}^{\mathrm{C}} (\gamma_{31} + \gamma_{32} + \gamma_{33})^2 . \tag{13}$$

Iso-biaxial stress in <111> fiber texture

In the case of <111> fiber texture material, <111> axes of crystals are preferred in the direction of specimen surface. In the other word, C coordinate system cannot be fixed. Therefore, the measurement strain $\overline{\varepsilon_{33}^{\mathrm{L}}}$ must be the average of normal strain affects on the diffraction $\overline{\varepsilon_{33}^{\mathrm{L}}}$. The equation 6 is applied the average of strain $\overline{\varepsilon_{33}^{\mathrm{L}}}$, transformed equation is given by

$$\overline{\varepsilon_{33}^{\mathrm{L}}} = (S_0^{\mathrm{C}} \overline{M_{ij}} + S_{12}^{\mathrm{C}}\delta_{ij} + \frac{1}{2} S_{44}^{\mathrm{C}} \omega_{3i}\omega_{3j})\sigma_{ij}^{\mathrm{P}} . \tag{14}$$

Here, assuming that the stress state has the iso-biaxial stress (substitute $\phi = 0$), the plane stress ($\sigma_{3i}^{\mathrm{P}} = 0$), and the <111> fiber texture material, the equation satisfied with these condition is as

$$\frac{\overline{\varepsilon_{33}^{\mathrm{L}}}}{\sigma^{\mathrm{P}}} = S_0^{\mathrm{C}}(\overline{M_{11}} + \overline{M_{22}}) + 2S_{12}^{\mathrm{C}} + \frac{1}{2}S_{44}^{\mathrm{C}}\sin^2\psi = \frac{2}{3}S_0^{\mathrm{C}} + 2S_{12}^{\mathrm{C}} + \frac{1}{2}S_{44}^{\mathrm{C}}\sin^2\psi \quad (15)$$

Explaining in addition, the transformation matrix π_{ij} is given as

$$\pi_{ij} = \begin{pmatrix} \frac{\cos\gamma}{\sqrt{6}} - \frac{\sin\gamma}{\sqrt{2}} & \frac{\cos\gamma}{\sqrt{6}} + \frac{\sin\gamma}{\sqrt{2}} & -\sqrt{\frac{2}{3}}\cos\gamma \\ -\frac{\sin\gamma}{\sqrt{6}} - \frac{\cos\gamma}{\sqrt{2}} & -\frac{\sin\gamma}{\sqrt{6}} + \frac{\cos\gamma}{\sqrt{2}} & \sqrt{\frac{2}{3}}\sin\gamma \\ \frac{1}{\sqrt{3}} & \frac{1}{\sqrt{3}} & \frac{1}{\sqrt{3}} \end{pmatrix}, \quad (16)$$

where γ is rotation angle around P_3 axis. In the <111> preferred orientation, angle γ is irrelevant to the equation 15.

Aniso-biaxial stress in <111> fiber texture

Equation 15 is assumed iso-biaxial stress state. Generally speaking, it is reported that thin films made by deposition process have iso-biaxial stress state (Tanaka and Ishihara, 1995). However, in this research, it is a possibility that a specimen has an aniso-biaxial stress due to deviated texture state. Then, aniso-biaxial stress analysis for cubic thin films provided by Tanaka et al. (1999) was applied. The stress-strain relation is described as

$$\begin{aligned}\varepsilon_{33}^{\mathrm{L}} = \{&\frac{1}{4}S_{44}(\sigma_{11}+\sigma_{22}) + \frac{1}{12}(3S_{44}+2S_0)(\sigma_{11}-\sigma_{22})\cos 2\phi + 2\sigma_{12}\sin 2\phi\}\sin^2\psi \\ &-\frac{\sqrt{2}}{6}S_0\{(\sigma_{11}-\sigma_{22})\cos(\phi+3\gamma) - 2\sigma_{12}\sin(\phi+3\gamma)\}\sin 2\psi \\ &+\frac{1}{3}(3S_{12}+S_0)(\sigma_{11}+\sigma_{22})\end{aligned} \quad (17)$$

Here, $\phi = 0$ and $\phi = 90$ is substituted respectively in equation 17, provided that angle γ has to be replaced with $\gamma - 90$. In addition, next equation is applied the average of strain $\varepsilon_{33}^{\mathrm{L}}$ like equation 14.

$$\begin{aligned}\overline{\varepsilon_{33}^{\mathrm{L}}}(\phi=0) = &\frac{1}{6}\{(3S_{44}+S_0)\sigma_{11} - S_0\sigma_{22}\}\sin^2\psi \\ &-\frac{\sqrt{2}}{6}S_0\{(\sigma_{11}-\sigma_{22})\overline{\cos 3\gamma} - 2\sigma_{12}\overline{\sin 3\gamma}\}\sin 2\psi \\ &+\frac{1}{3}(3S_{12}+S_0)(\sigma_{11}+\sigma_{22})\end{aligned}, \quad (18)$$

$$\begin{aligned}\overline{\varepsilon_{33}^{\mathrm{L}}}(\phi=90) = &\frac{1}{6}\{-S_0\sigma_{11} - (3S_{44}+S_0)\sigma_{22}\}\sin^2\psi \\ &+\frac{\sqrt{2}}{6}S_0\{(\sigma_{11}-\sigma_{22})\overline{\cos 3\gamma} - 2\sigma_{12}\overline{\sin 3\gamma}\}\sin 2\psi \\ &+\frac{1}{3}(3S_{12}+S_0)(\sigma_{11}+\sigma_{22})\end{aligned}. \quad (19)$$

$\overline{\cos 3\gamma}$ and $\overline{\sin 3\gamma}$ can be decided by measurement plane. If the plane is chosen under the condition that $\cos 3\gamma = \sin 3\gamma = 0$ successfully, stress calculation can be done using the equation differentiated by $\sin^2\psi$.

EXPERIMENTS

Specimen preparation

TiN thin film was deposited by PVD on a JIS-SKH51 (AISI-M2) steel substrate. The substrate has dimensions of 18mm diameter and 10mm height. On the condition of PVD, processing gas was used N_2 gas in the pressure about 0.4Pa. The substrate bias voltage was –80V, and the arc current was 80A. The thickness of film was about 2.5μm.

Pole figure measurement and stress measurement

The pole figure was measured using Cu-Kα radiation with Schulz reflection method to evaluate the texture state in thin film (Gotoh et al., 2003). The schematic illustrations and a photograph are shown in figure 3. On measurement conditions, the X-ray tube voltage was 40kV and the tube current was 200mA. The inclination angle normal to the specimen surface α was changed from 90 to 15deg in intervals of 15deg, and the rotation angle β was changed from 0 to 355deg in intervals of 5deg. Here, two angles α and β are corresponded with $\psi = 90 - \alpha$ and $\phi = \beta$ respectively. {111}, {100}, {110}, {311} and {210} were measured.

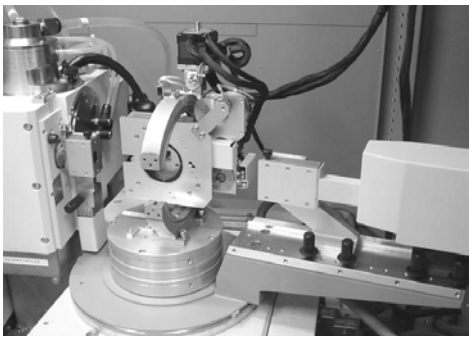

(a) Photograph of measurement equipment.

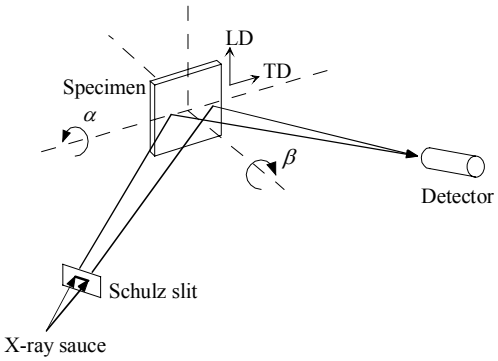

(b) Optics of pole figure measurement.

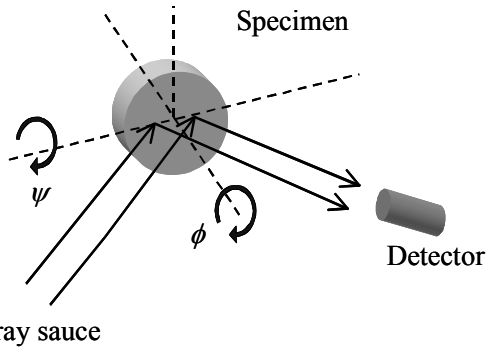

(c) Optics of stress measurement.

Fig. 3 Schematic illustration and a photograph of measurement system.

The stress measurement (Gotoh et al., 2002) was also executed using Cu-Kα radiation. The tube voltage and current were just like pole figure measurement. Parallel beam optics was applied in measurement. Ni foil was used as a Kβ radiation filter. The integrated intensity of diffraction profile was measured to correct ϕ position exactly. Here, the elastic compliance moduli of TiN (Perry, 1989) used in stress analysis was

$$S_{11}^{\mathrm{C}} = 2.17\ ,\ S_{12}^{\mathrm{C}} = -0.38\ ,\ S_{44}^{\mathrm{C}} = 5.95\ \ \mathrm{TPa}^{-1}. \tag{20}$$

In this stress measurement, stress-free lattice spacing d_0 is need to calculate the strain $\varepsilon_{33}^{\mathrm{L}}$ obtained by peak shift of X-ray profile. $\varepsilon_{33}^{\mathrm{L}}$ can be calculated by

$$\varepsilon_{33}^{\mathrm{L}} = \frac{d - d_0}{d_0}, \tag{21}$$

where d is the lattice spacing obtained by Bragg's law $2d\sin\theta = n\lambda$, and d_0 also can be obtained by Bragg's law similarly. However, it is well understood by equation 21 that correct measurement of $\varepsilon_{33}^{\mathrm{L}}$ is accomplished by exact measurement of d_0. Therefore, it is preferable not to use d_0 in stress measurement. Thus, two-exposure method (Ejiri et al., 2000) was applied to this study. Here, if equation 21 is applied to equation 13 and 15, they may be expressed as following form:

$$d = d_0(S\sigma^{P} + 1)\,. \tag{22}$$

S represents the right-hand side of equation 13 and 15. Here, if the diffraction plane about d_1 and d_2 can be selected in the plane having same stress-free lattice spacing d_0, (in the other word: in case of having same d_0 in different angle ψ or different *hkl*), two measured value (d_1, S_1) and (d_2, S_2) become the simultaneous equations of $(\sigma^{\mathrm{P}}, d_0)$. Therefore, σ^{P} is given by

$$\sigma^{\mathrm{P}} = \frac{d_2 - d_1}{d_1 S_2 - d_2 S_1}\,. \tag{23}$$

Thus, the stress σ^{P} can be obtained by d spacing measurement and S calculation using stress-strain relation procedure without d_0.

RESULTS AND DISCUSSION

Figure 4 shows pole figures obtained in this study. In the figure 4(b) and 4(c), three high intensity spots appear in spread circular line. In the case of single crystal, only spots should be appeared clearly. Otherwise, in the ideal fiber texture, it should be indicated shallower spread circular line without spots (Gotoh et al., 2003). Therefore, in this specimen, it shows medium property between the single crystal and the fiber texture. However, in the figure 4(d) and 4(e), spots could not be observed. It is thought the large multiplicity factor of {311} and {210} contributes to the swing of C axes. Thus, diffraction might get blurred. <111> preferred orientation in this thin film was understood by all pole figures obtained from each planes.

An example of X-ray diffraction profile used in stress measurement is shown in figure 5. The profile was symmetrical, and it was reliable to measure the stress.

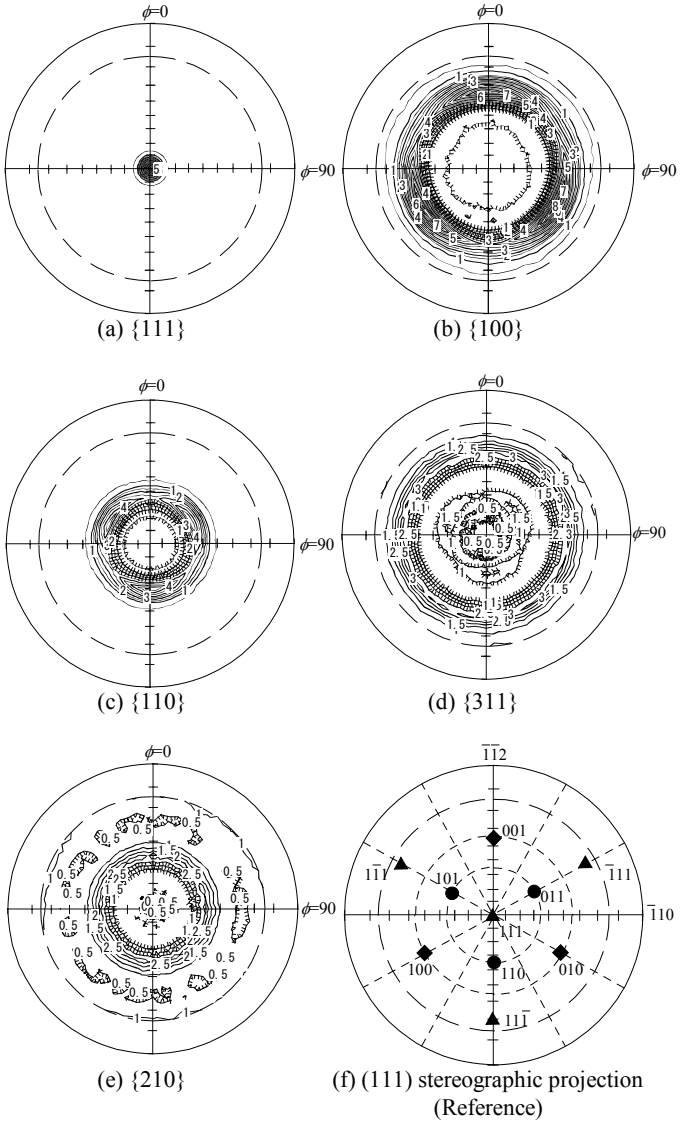

Fig. 4 Pole figures and a stereographic projection of cubic single crystal.

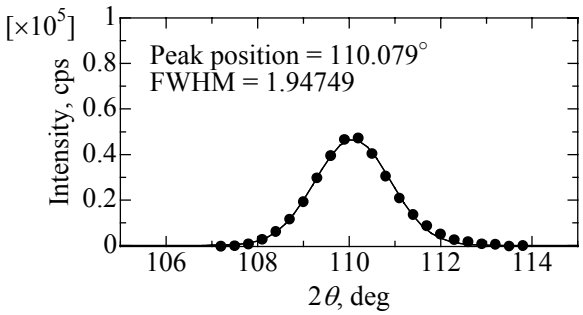

Fig. 5 Example of peak profile (042 plane).

Concerning stress measurement, at first, stresses were measured with equation 13 by using several diffraction planes shown in figure 6. Results are listed in table 1. The thin film had about 6GPa compressive residual stress. However, a little difference was at each plane.

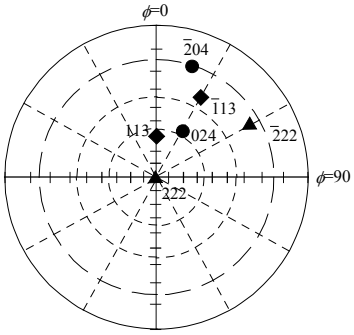

Fig. 6 Measurement positions and planes.

Next, in (222) and (420) diffraction in figure 6, an influence of miss-positioning about angle ϕ was evaluated. The concept of this measurement concerning miss-positioning error is shown in figure 7. For example, ideal position of 222 diffraction plane is $\phi = 60$, however, the stress was measured at ideal position and the stress was also calculated by using missed position of 222 plane at $\phi = 0$. Thus, stresses were compared. As results, there was no difference in 222 plane, however, diffraction intensity at right position was the twice as large as that of missed position. Otherwise, a little difference was in 420 plane. Residual stress at $\phi = 0$ (missed position) using 420 plane was -5.449GPa, it was more little than that in table 1. Now, equation 13 and 15 are assumed the ideal orientation. However, it was understood that the 420 diffraction was isotropic by figure 4(e). Therefore, it is thought that deviated error from ideal model was occurred. Here, relation between S ($= \varepsilon_{33}^{L} / \sigma^{P}$) and $\sin^2\psi$ using equation 15 is shown in figure 8. The solid line and the broken line are the elastic compliance of iso-biaxial random orientation model (Reuss model). At (222) and $(\bar{2}\bar{2}\bar{2})$ plane, the circle marks are on the solid line of 222 plane. However, the square mark of (420) plane (solid square mark) is a little away from the broken line of 420 plane. Thus, in the measurement using 420 plane, stress-strain relation by <111> ideal fiber model is not suitable. And it is seemed that the measurement using {111} planes in <111> fiber texture material accomplishes little error measurement.

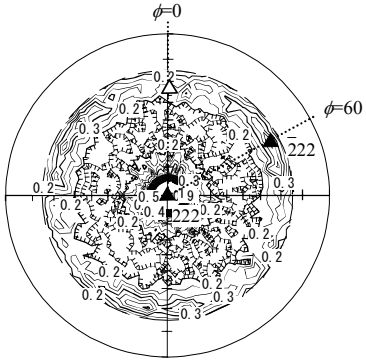

Fig. 7 Positions of miss-orientation measurement at (222).

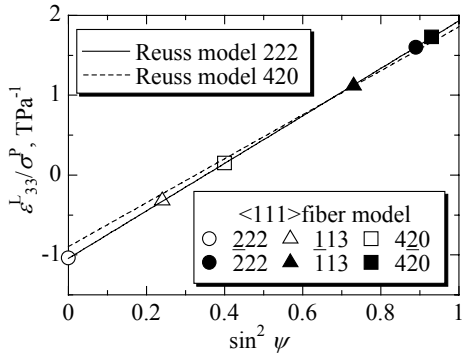

Fig.8 Relation between $\varepsilon_{33}^{L} / \sigma^{P}$ and $\sin^2\psi$.

At last, aniso-biaxial stress state was analyzed using equation 18 and 19. Measurement points were shown in figure 9. Here, because the planes are at $\phi = 0$ and $\phi = 90$, the relation $\cos 3\gamma = \sin 3\gamma = 0$ is adapted in equation 18 and 19. And simultaneous equations are obtained by equation 18 and 19 as follows:

$$\frac{\partial\{[\varepsilon_{33}^{L}(\phi=0)+\varepsilon_{33}^{L}(\phi=90)]/2\}}{\partial \sin^2\psi} = \frac{1}{4} S_{44}^{C}(\sigma_{11}+\sigma_{22}), \tag{17}$$

$$\frac{\partial \varepsilon_{33}^{L}(\phi=90)}{\partial \sin^2\psi} = \frac{1}{6}\{-S_0^{C}\sigma_{11} + (3S_{44}^{C}+S_0^{C})\sigma_{22}\}. \tag{18}$$

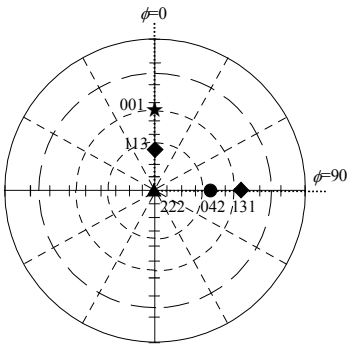

Fig. 9 Measurement positions and planes in aniso-biaxial stress analysis.

Table 1. Results of stress measurement using equation 13.

Plane	Stress, GPa
222	-5.881
113	-5.776
042	-5.531

Table 2. Results of stress measurement using equation 18 and 19.

Plane stress	Stress, GPa
σ_{11}	-6.49
σ_{22}	-6.10

By gradient in relation between ε_{33}^{L} and $\sin^2\psi$ ($\sin^2\psi$ plot diagram), the stress σ_{11} and σ_{22} can be obtained individually. Here, because ε_{33}^{L} is calculated by equation 21, stress-free lattice spacing d_0 is needed. Results are listed in table 2. σ_{11} was a little different from σ_{22}. It is though that this difference is occurred because of experimental error of d_0. Therefore, this thin film should have iso-biaxial stress state. In addition, stresses were lager than those of table 1. In the stress analysis at table 1, d_0 should not influence on the stress because of using two-exposure method. Therefore, it is thought stresses are get confused by the large multiplicity factors excepted for 222 plane just like pole figure measurement and stress measurement using equation 17 and 18.

CONCLUSIONS

Main results in this study are summarized as following:

(1) Specimen had compressive residual stress about –6GPa. Differences of stress value due to diffraction planes are in the measurement using the single crystal model and the ideal fiber texture model, and they were also in the measurement using aniso-biaxial model.

(2) By stress measurement assumed normal plane stress, the stress value was evaluated. As a result, this thin film has bi-axial stress state.

REFERRENCES

Brückner, U, Epishin, A, Link, T, Fedelich, B, Portella, PD (2005). "Dendritic Stresses in Nickel-Base Superalloys", *Material Science Forum*, Vols 490-491, pp.497-502.

Ejiri, S, He, T, Sasaki, T and Hirose, Y (2000). "X-Ray Stress Measurement for <110>-Oriented TiC Films", *Material Science Research International*, Vol 6, No 4, pp.237-242.

Gotoh, M, Murotani, T, Sasaki, T, Hirose, Y (2002). "X-ray Stress Measurements of TiCN Thin Films", *Material Science Forum*, Vols 404-407, pp.677-682.

Gotoh, M, Sasaki, T, Hirose, H (2003). "Changes of Crystallite Orientation Distribution in TiCN Thin Films due to Bias Voltages", *Proceedings of The Thirteenth International Offshore and Polar Engineering Conference*, Vol 4, pp.185-189.

Kittel, C (1996). "Introduction to Solid State Physics 7th Edition", John Wiley & Sons, Inc. New York

Ma, CH, Huang, JH, Chen, H (2002). "Residual Stress Measurement in Textured Thin Film by Grazing-incidence X-ray Diffraction", *Thin Solid Films*, Vol 418, pp.73-78.

Miki, Y, Taniguchi, T, Hanabusa, T, Kusaka, K and Matsue, T (2000). "X-Ray Stress Measurement and Mechanical Properties of TiN Films Coated on Aluminum and Aluminum Alloy Substrates by Arc Ion Plating and Ion Beam Mixing", *Material Science Research International*, Vol 6, No 4, pp.243-248.

Murotani, T, Hirose, H, Sasaki, T, Okazaki, K (2000). "Study on stress measurement of PVD-coating layer", *Thin Solid Films*, Vol 377-378, pp.617-620.

Noyan, IC and Cohen, JB (1987). "Residual stress", Springer-Verlag New York

Perry, AJ (1989). "The Relationship Between Residual Stress X-ray Elastic Constants and Lattice Parameters in TiN Films Made by Physical Vapor Deposition", *Thin Solid Films*, Vol 170, pp.63-70.

Scardi, P, Dong, Y, H (2001). "Residual Stress in Fiber-textured Thin Films of Cubic Materials", *Journal of Materials Research*, Vol 16, pp.233-242.

Suzuki, H, Akita, K, Misawa, H (2000). "X-Ray Stress Measurement of Silicon Single Crystal", *Material Science Research International*, Vol 6, No 4, pp.255-262.

Suzuki, H, Akita, K, Misawa, H (2003). "X-Ray Stress Measurement Method for Single Crystal with Unknown Stress-Free Lattice Parameter", *Japanese Journal of Applied Physics*, Vol 42, No 5A, pp.2876-2880.

Tanaka, K, Ishihara, K (1995). "X-Ray Stress Measurement of Aluminum Thin Films Sputtered on Silicon Wafers", *Transaction of the Japan society of mechanical engineering*, Vol 61, No 589, pp.1971-1978.

Tanaka, K, Akiniwa, Y, Ito, T, Inoue, K (1999). "Elastic Constants and X-Ray Stress Measurement of Cubic Thin Films with Fiber Texture", *JSME International Journal Series A*, Vol 42, No 2, pp.224-234.

Tanaka, K, Ito, T, Akiniwa, Y, Kimachi, H, Miki, Y (2000). "X-Ray Stress Measurement of TiN Thin Film with <110> Fiber Texture under External Loading", *Material Science Research International*, Vol 6, No 4, pp.231-236.

Tanaka, K, Ito, T, Akiniwa, Y, Kimachi, H, Miki, Y (2000). "X-Ray Stress Measurement of TiN Thin Film with <110> Fiber Texture under External Loading", *Material Science Research International*, Vol 6, No 4, pp.231-236.

Zaouali, Z, Lebrun, JL, Gergaud, P (1991). "X-ray Diffraction Determination of Texture and Internal Stresses in Magnetron PVD Molybdenum Thin Films", *Surface and Coatings Technology*, Vol 50, pp.5-10.